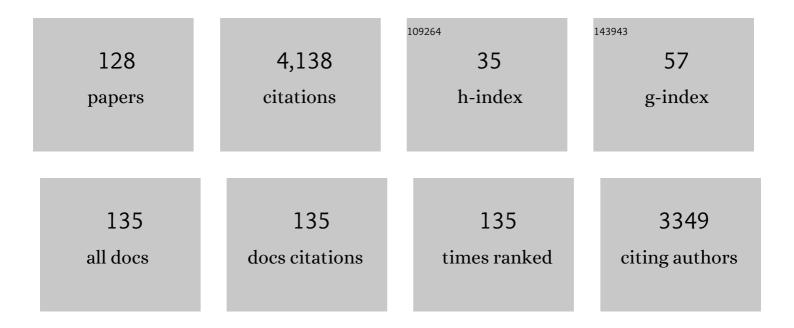
List of Publications by Year in descending order

Source: https://exaly.com/author-pdf/4327607/publications.pdf Version: 2024-02-01



LILLEN TRÃ OROSC

#	Article	IF	CITATIONS
1	Solid-State NMR Study of MCM-41-type Mesoporous Silica Nanoparticles. Journal of the American Chemical Society, 2005, 127, 3057-3068.	6.6	235
2	Geometry Flexibility of Copper Iodide Clusters: Variability in Luminescence Thermochromism. Inorganic Chemistry, 2015, 54, 4483-4494.	1.9	136
3	Proton-detected 14N MAS NMR using homonuclear decoupled rotary resonance. Chemical Physics Letters, 2007, 435, 163-169.	1.2	135
4	Broadband homonuclear correlation spectroscopy driven by combined <mml:math xmlns:mml="http://www.w3.org/1998/Math/MathML" altimg="si1.gif" overflow="scroll"&gt;<mml:mrow><mml:mtext>R</mml:mtext><mml:msubsup><mml:mrow><mml:mn>2sequences under fast magic angle spinning for NMR structural analysis of organic and biological solids. Journal of Magnetic Resonance, 2013, 232, 18-30.</mml:mn></mml:mrow></mml:msubsup></mml:mrow></mml:math 	mn>1./2nml:	mr <b>aø</b> 2 < mml:
5	Measurement of hetero-nuclear distances using a symmetry-based pulse sequence in solid-state NMR. Physical Chemistry Chemical Physics, 2010, 12, 9395.	1.3	120
6	Recent developments in MAS DNP-NMR of materials. Solid State Nuclear Magnetic Resonance, 2019, 101, 116-143.	1.5	116
7	Beyond the Silica Surface by Direct Siliconâ€⊋9 Dynamic Nuclear Polarization. Angewandte Chemie - International Edition, 2011, 50, 8367-8370.	7.2	115
8	Studies of Organically Functionalized Mesoporous Silicas Using Heteronuclear Solid-State Correlation NMR Spectroscopy under Fast Magic Angle Spinning. Journal of the American Chemical Society, 2005, 127, 7587-7593.	6.6	113
9	Chemical bonding differences evidenced from J-coupling in solid state NMR experiments involving quadrupolar nuclei. Journal of Magnetic Resonance, 2003, 164, 160-164.	1.2	110
10	BrÃ,nsted acid sites based on penta-coordinated aluminum species. Nature Communications, 2016, 7, 13820.	5.8	99
11	Boron isotopes as pH proxy: A new look at boron speciation in deep-sea corals using 11B MAS NMR and EELS. Geochimica Et Cosmochimica Acta, 2011, 75, 1003-1012.	1.6	94
12	<sup>17</sup> 0 NMR Gives Unprecedented Insights into the Structure of Supported Catalysts and Their Interaction with the Silica Carrier. Journal of the American Chemical Society, 2012, 134, 9263-9275.	6.6	93
13	Heteronuclear NMR Spectroscopy as a Surfaceâ€Selective Technique: A Unique Look at the Hydroxyl Groups of γâ€Alumina Chemistry - A European Journal, 2014, 20, 4038-4046.	1.7	82
14	Indirect Detection via Spin-1/2 Nuclei in Solid State NMR Spectroscopy: Application to the Observation of Proximities between Protons and Quadrupolar Nuclei. Journal of Physical Chemistry A, 2009, 113, 12864-12878.	1.1	81
15	The acidic nature of "NMR-invisible―tri-coordinated framework aluminum species in zeolites. Chemical Science, 2019, 10, 10159-10169.	3.7	78
16	Probing <sup>27</sup> Al– <sup>13</sup> C proximities in metal–organic frameworks using dynamic nuclear polarization enhanced NMR spectroscopy. Chemical Communications, 2014, 50, 933-935.	2.2	67
17	Indirect and direct <sup>29</sup> Si dynamic nuclear polarization of dispersed nanoparticles. Chemical Communications, 2013, 49, 2864-2866.	2.2	62
18	Distance measurement between a spin-1/2 and a half-integer quadrupolar nuclei by solid-state NMR using exact analytical expressions. Journal of Magnetic Resonance, 2010, 206, 269-273.	1.2	61

#	Article	IF	CITATIONS
19	Enhanced resolution in proton solid-state NMR with very-fast MAS experiments. Journal of Magnetic Resonance, 2008, 193, 305-307.	1.2	60
20	Measurement of Aluminum–Carbon Distances Using Sâ€RESPDOR NMR Experiments. ChemPhysChem, 2012, 13, 3605-3615.	1.0	59
21	Synergic Effect of Active Sites in Zincâ€Modified ZSMâ€5 Zeolites as Revealed by Highâ€Field Solidâ€State NMR Spectroscopy. Angewandte Chemie - International Edition, 2016, 55, 15826-15830.	7.2	59
22	Broad-band homo-nuclear correlations assisted by 1H irradiation for bio-molecules in very high magnetic field at fast and ultra-fast MAS frequencies. Journal of Magnetic Resonance, 2011, 212, 320-329.	1.2	55
23	Detailed analysis of the S-RESPDOR solid-state NMR method for inter-nuclear distance measurement between spin-1/2 and quadrupolar nuclei. Journal of Magnetic Resonance, 2012, 215, 34-49.	1.2	52
24	The D-HMQC MAS-NMR Technique. Annual Reports on NMR Spectroscopy, 2014, , 145-184.	0.7	52
25	A well-defined silica-supported aluminium alkyl through an unprecedented, consecutive two-step protonolysis–alkyl transfer mechanism. Chemical Communications, 2011, 47, 2979.	2.2	51
26	Heteronuclear NMR Correlations To Probe the Local Structure of Catalytically Active Surface Aluminum Hydride Species on γâ€Alumina. Angewandte Chemie - International Edition, 2010, 49, 9854-9858.	7.2	47
27	Modification of Molybdenum Structural Environment in Borosilicate Glasses with Increasing Content of Boron and Calcium Oxide by <scp><scp><sup>95</sup>Mo</scp> MAS NMR</scp> . Journal of the American Ceramic Society, 2011, 94, 4274-4282.	1.9	45
28	Q-shear transformation for MQMAS and STMAS NMR spectra. Journal of Magnetic Resonance, 2009, 201, 81-86.	1.2	43
29	SPAM-MQ-HETCOR: an improved method for heteronuclear correlation spectroscopy between quadrupolar and spin-1/2 nuclei in solid-state NMR. Physical Chemistry Chemical Physics, 2006, 8, 144-150.	1.3	41
30	High-resolution through-space correlations between spin-1/2 and half-integer quadrupolar nuclei using the MQ-D-R-INEPT NMR experiment. Physical Chemistry Chemical Physics, 2012, 14, 7112.	1.3	41
31	Practical choice of 1H–1H decoupling schemes in through-bond 1H–{X} HMQC experiments at ultra-fast MAS. Journal of Magnetic Resonance, 2012, 214, 151-158.	1.2	41
32	On the Track to Silica-Supported Tungsten Oxo Metathesis Catalysts: Input from <sup>17</sup> O Solid-State NMR. Inorganic Chemistry, 2013, 52, 10119-10130.	1.9	40
33	Acidity enhancement through synergy of penta- and tetra-coordinated aluminum species in amorphous silica networks. Nature Communications, 2020, 11, 225.	5.8	40
34	Broadband finite-pulse radio-frequency-driven recoupling (fp-RFDR) with (XY8)41 super-cycling for homo-nuclear correlations in very high magnetic fields at fast and ultra-fast MAS frequencies. Journal of Magnetic Resonance, 2012, 223, 107-119.	1.2	37
35	Observation of Low-Î <sup>3</sup> Quadrupolar Nuclei by Surface-Enhanced NMR Spectroscopy. Journal of the American Chemical Society, 2020, 142, 10659-10672.	6.6	36
36	High-Resolution Structural Characterization of Two Layered Aluminophosphates by Synchrotron Powder Diffraction and NMR Crystallographies. Chemistry of Materials, 2013, 25, 2227-2242.	3.2	35

#	Article	IF	CITATIONS
37	Homonuclear dipolar recoupling under ultra-fast magic-angle spinning: Probing 19Fâ^'19F proximities by solid-state NMR. Journal of Magnetic Resonance, 2010, 203, 113-128.	1.2	34
38	A Study of Transitionâ€Metal Organometallic Complexes Combining <sup>35</sup> Cl Solid‣tate NMR Spectroscopy and <sup>35</sup> Clâ€NQR Spectroscopy and Firstâ€Principles DFT Calculations. Chemistry - A European Journal, 2013, 19, 12396-12414.	1.7	34
39	Signal enhancement of J-HMQC experiments in solid-state NMR involving half-integer quadrupolar nuclei. Chemical Communications, 2013, 49, 6653.	2.2	34
40	An NMRâ€Driven Crystallography Strategy to Overcome the Computability Limit of Powder Structure Determination: A Layered Aluminophosphate Case. Chemistry - A European Journal, 2013, 19, 5009-5013.	1.7	34
41	Solvent-Free High-Field Dynamic Nuclear Polarization of Mesoporous Silica Functionalized with TEMPO. Applied Magnetic Resonance, 2012, 43, 237-250.	0.6	33
42	Comparison of high-resolution solid-state NMR MQMAS and STMAS methods for half-integer quadrupolar nuclei. Solid State Nuclear Magnetic Resonance, 2007, 31, 1-9.	1.5	31
43	Host–Guest Interactions in Dealuminated HY Zeolite Probed by <sup>13</sup> C– <sup>27</sup> Al Solid-State NMR Spectroscopy. Journal of Physical Chemistry Letters, 2014, 5, 3068-3072.	2.1	31
44	Double-quantum 19F–19F dipolar recoupling at ultra-fast magic angle spinning NMR: application to the assignment of 19F NMR spectra of inorganic fluorides. Physical Chemistry Chemical Physics, 2009, 11, 10391.	1.3	30
45	Indirect high-resolution detection for quadrupolar spin-3/2 nuclei in dipolar HMQC solid-state NMR experiments. Chemical Physics Letters, 2010, 496, 201-207.	1.2	30
46	A tunable homonuclear dipolar decoupling scheme for high-resolution proton NMR of solids from slow to fast magic-angle spinning. Chemical Physics Letters, 2011, 503, 167-170.	1.2	30
47	Uniform broadband excitation of crystallites in rotating solids using interleaved sequences of delays alternating with nutation. Journal of Magnetic Resonance, 2012, 223, 228-236.	1.2	29
48	Population transfer HMQC for half-integer quadrupolar nuclei. Journal of Chemical Physics, 2015, 142, 094201.	1.2	29
49	An Investigation of Chlorine Ligands in Transition-Metal Complexes via <sup>35</sup> Cl Solid-State NMR and Density Functional Theory Calculations. Inorganic Chemistry, 2014, 53, 9581-9597.	1.9	28
50	Homonuclear dipolar decoupling schemes for fast MAS. Solid State Nuclear Magnetic Resonance, 2009, 35, 19-24.	1.5	26
51	Measurement of 13C–1H dipolar couplings in solids by using ultra-fast magic-angle spinning NMR spectroscopy with symmetry-based sequences. Physical Chemistry Chemical Physics, 2011, 13, 5967.	1.3	25
52	Solid-state NMR indirect detection of nuclei experiencing large anisotropic interactions using spinning sideband-selective pulses. Solid State Nuclear Magnetic Resonance, 2015, 72, 104-117.	1.5	25
53	Solid-state NMR covariance of homonuclear correlation spectra. Journal of Chemical Physics, 2008, 128, 134502.	1.2	24
54	Boron Nitride and Oxide Supported on Dendritic Fibrous Nanosilica for Catalytic Oxidative Dehydrogenation of Propane. ACS Sustainable Chemistry and Engineering, 2020, 8, 16124-16135.	3.2	23

#	Article	IF	CITATIONS
55	Detailed analysis of the TIMES and TIMESO high-resolution MAS methods for high-resolution proton NMR. Journal of Magnetic Resonance, 2012, 223, 219-227.	1.2	22
56	Advances in Structural Studies on Alkylaluminum Species in the Solid State via Challenging 27Al–13C NMR Spectroscopy and X-ray Diffraction. Journal of Physical Chemistry C, 2013, 117, 18091-18099.	1.5	22
57	NMR crystallography to probe the breathing effect of the MIL-53(Al) metal–organic framework using solid-state NMR measurements of <sup>13</sup> C– <sup>27</sup> Al distances. Acta Crystallographica Section C, Structural Chemistry, 2017, 73, 176-183.	0.2	22
58	3D 1H–13C–14N correlation solid-state NMR spectrum. Journal of Magnetic Resonance, 2008, 193, 321-325.	1.2	21
59	Proton-proton homonuclear dipolar decoupling in solid-state NMR using rotor-synchronized z-rotation pulse sequences. Journal of Chemical Physics, 2009, 130, 014504.	1.2	21
60	Broadband excitation in solid-state NMR using interleaved DANTE pulse trains with N pulses per rotor period. Journal of Magnetic Resonance, 2013, 236, 105-116.	1.2	21
61	NMR Crystallography of an Oxovanadium(V) Complex by an Approach Combining Multinuclear Magic Angle Spinning NMR, DFT, and Spin Dynamics Simulations. ChemPhysChem, 2015, 16, 1619-1626.	1.0	21
62	Magnetization transfer from protons to quadrupolar nuclei in solid-state NMR using PRESTO or dipolar-mediated refocused INEPT methods. Journal of Magnetic Resonance, 2019, 299, 109-123.	1.2	21
63	Broadband excitation in solid-state NMR of paramagnetic samples using Delays Alternating with Nutation for Tailored Excitation (†Para-DANTE'). Chemical Physics Letters, 2012, 553, 68-76.	1.2	20
64	Structural Study of Mg-Based Metal–Organic Frameworks by X-ray Diffraction, 1H, 13C, and 25Mg Solid-State NMR Spectroscopy, and First-Principles Calculations. Journal of Physical Chemistry C, 2015, 119, 7831-7841.	1.5	20
65	Very‣ongâ€Distance Correlations in Proteins Revealed by Solidâ€State NMR Spectroscopy. ChemPhysChem, 2012, 13, 3585-3588.	1.0	19
66	Analysis of local molecular motions of aromatic sidechains in proteins by 2D and 3D fast MAS NMR spectroscopy and quantum mechanical calculations. Physical Chemistry Chemical Physics, 2015, 17, 28789-28801.	1.3	19
67	Solidâ€State NMR Spectroscopy Proves the Presence of Pentaâ€coordinated Sc Sites in MILâ€100(Sc). Chemistry - A European Journal, 2017, 23, 9525-9534.	1.7	19
68	Study of Xenon Mobility in the Two Forms of MIL-53(Al) Using Solid-State NMR Spectroscopy. Journal of Physical Chemistry C, 2017, 121, 19262-19268.	1.5	19
69	1H–1H double-quantum CRAMPS NMR at very-fast MAS (μ⁄2R=35kHz): A resolution enhancement method to probe 1H–1H proximities in solids. Journal of Magnetic Resonance, 2009, 196, 88-91.	1.2	18
70	Observing 13C–13C connectivities at high magnetic fields and very high spinning frequencies. Chemical Communications, 2011, 47, 6930.	2.2	18
71	Comparison of various NMR methods for the indirect detection of nitrogen-14 nuclei via protons in solids. Journal of Magnetic Resonance, 2015, 258, 86-95.	1.2	18
72	A soft-chemistry approach to the synthesis of amorphous calcium ortho/pyrophosphate biomaterials of tunable composition. Acta Biomaterialia, 2020, 103, 333-345.	4.1	18

#	Article	IF	CITATIONS
73	Imaging the spatial distribution of radiofrequency field, sample and temperature in MAS NMR rotor. Solid State Nuclear Magnetic Resonance, 2017, 87, 137-142.	1.5	17
74	Observation of proximities between spin-1/2 and quadrupolar nuclei in solids: Improved robustness to chemical shielding using adiabatic symmetry-based recoupling. Solid State Nuclear Magnetic Resonance, 2018, 94, 7-19.	1.5	16
75	Efficiency at high spinning frequencies of heteronuclear decoupling methods designed to quench rotary resonance. Solid State Nuclear Magnetic Resonance, 2011, 40, 21-26.	1.5	15
76	Quantitative cross-polarization at magic-angle spinning frequency of about 20kHz. Journal of Magnetic Resonance, 2012, 214, 340-345.	1.2	15
77	Evaluation of excitation schemes for indirect detection of 14N via solid-state HMQC NMR experiments. Journal of Magnetic Resonance, 2019, 303, 28-41.	1.2	15
78	Î <sup>3</sup> -Independent through-space hetero-nuclear correlation between spin-1/2 and quadrupolar nuclei in solids. Solid State Nuclear Magnetic Resonance, 2017, 84, 216-226.	1.5	14
79	Recent Developments in NMR Studies of Aluminophosphates. Annual Reports on NMR Spectroscopy, 2018, 94, 113-185.	0.7	14
80	Analysis of HMQC experiments applied to a spin ½ nucleus subject to very large CSA. Solid State Nuclear Magnetic Resonance, 2019, 100, 11-25.	1.5	14
81	Indirect covariance NMR spectroscopy of through-bond homo-nuclear correlations for quadrupolar nuclei in solids under high-resolution. Solid State Nuclear Magnetic Resonance, 2007, 31, 163-168.	1.5	13
82	Comparison of various sampling schemes and accumulation profiles in covariance spectroscopy with exponentially decaying 2D signals. Analyst, The, 2013, 138, 2411.	1.7	13
83	gem â€Diolâ€Type Intermediate in the Activation of a Ketone on Snâ€Î² Zeolite as Studied by Solidâ€State NMR Spectroscopy. Angewandte Chemie - International Edition, 2020, 59, 19532-19538.	7.2	13
84	A New Donor‣tabilized Ditungsten Amido Alkoxido Species: Synthesis, Crystal Structure, Fluxionality, and Grafting onto Silica. European Journal of Inorganic Chemistry, 2007, 2007, 5541-5547.	1.0	12
85	<sup>95</sup> Mo Solid-State Nuclear Magnetic Resonance Spectroscopy and Quantum Simulations: Synergetic Tools for the Study of Molybdenum Cluster Materials. Inorganic Chemistry, 2013, 52, 617-627.	1.9	12
86	Synergic Effect of Active Sites in Zincâ€Modified ZSMâ€5 Zeolites as Revealed by Highâ€Field Solidâ€State NMR Spectroscopy. Angewandte Chemie, 2016, 128, 16058-16062.	1.6	12
87	14N overtone nuclear magnetic resonance of rotating solids. Journal of Chemical Physics, 2018, 149, 064201.	1.2	12
88	High-resolution 14N-edited 1H–13C correlation NMR experiment to study biological solids. Journal of Magnetic Resonance, 2008, 194, 317-320.	1.2	11
89	Fast acquisition of multidimensional NMR spectra of solids and mesophases using alternative sampling methods. Magnetic Resonance in Chemistry, 2015, 53, 927-939.	1.1	11
90	Probing the aluminum complexation by Siberian riverine organic matter using solid-state DNP-NMR. Chemical Geology, 2017, 452, 1-8.	1.4	11

#	Article	IF	CITATIONS
91	Uniform signal enhancement in MAS NMR of half-integer quadrupolar nuclei using quadruple-frequency sweeps. Journal of Magnetic Resonance, 2018, 293, 92-103.	1.2	11
92	Caveat on the Actual Robustness of Heteronuclear NMR Methods for Probing the Surface of Î <sup>3</sup> -Alumina and Related Catalysts. Journal of Physical Chemistry C, 2019, 123, 12919-12927.	1.5	11
93	Rapid analysis of isotopically unmodified amino acids by high-resolution 14N-edited 1H–13C correlation NMR spectroscopy. Chemical Communications, 2008, , 6525.	2.2	10
94	Quantitative Analysis of the Proximities of OH Ligands and Vanadium Sites in a Polyoxovanadate Cluster Using Frequency-Selective 1H–51V Solid-State NMR Spectroscopy. Journal of Physical Chemistry C, 2014, 118, 18580-18588.	1.5	10
95	Indirect detection of broad spectra in solid-state NMR using interleaved DANTE trains. Journal of Magnetic Resonance, 2018, 294, 101-114.	1.2	10
96	Labeling and Probing the Silica Surface Using Mechanochemistry and 17 Oâ€NMR Spectroscopy**. Chemistry - A European Journal, 2021, 27, 12574-12588.	1.7	10
97	Indirect NMR detection via proton of nuclei subject to large anisotropic interactions, such as 14N, 195Pt, and 35Cl, using the T-HMQC sequence. Journal of Chemical Physics, 2022, 156, 064202.	1.2	10
98	Efficient transfer of DNPâ€enhanced <sup>1</sup> H magnetization to halfâ€integer quadrupolar nuclei in solids at moderate spinning rate. Magnetic Resonance in Chemistry, 2021, 59, 920-939.	1.1	9
99	NMR Crystallography Reveals Carbonate Induced Alâ€Ordering in ZnAl Layered Double Hydroxide. Chemistry - A European Journal, 2021, 27, 15944-15953.	1.7	9
100	I-STMAS, a new high-resolution solid-state NMR method for half-integer quadrupolar nuclei. Solid State Nuclear Magnetic Resonance, 2003, 23, 213-223.	1.5	8
101	Observation of 1H–13C and 1H–1H proximities in a paramagnetic solid by NMR at high magnetic field under ultra-fast MAS. Journal of Magnetic Resonance, 2015, 251, 36-42.	1.2	8
102	Highâ€field <sup>95</sup> Mo and <sup>183</sup> W static and MAS NMR study of polyoxometalates. Magnetic Resonance in Chemistry, 2017, 55, 902-908.	1.1	8
103	Improved sensitivity and quantification for 29Si NMR experiments on solids using UDEFT (Uniform) Tj ETQq1 1	0.784314	rgBT /Overloci
104	A comparison of through-space population transfers from half-integer spin quadrupolar nuclei to 1H using MQ-HETCOR and MQ-SPAM-HETCOR under fast MAS. Journal of Magnetic Resonance, 2021, 329, 107028.	1.2	8
105	Accelerating the acquisition of high-resolution quadrupolar MQ/ST-HETCOR 2D spectra under fast MAS via 1H detection and through-space population transfers. Journal of Magnetic Resonance, 2021, 333, 107093.	1.2	8
106	Revealing BrÃ,nsted Acidic Bridging SiOHAl Groups on Amorphous Silica–Alumina by Ultrahigh Field Solid-State NMR. Journal of Physical Chemistry Letters, 2021, 12, 11563-11572.	2.1	8
107	Improved NMR transfer of magnetization from protons to half-integer spin quadrupolar nuclei at moderate and high magic-angle spinning frequencies. Magnetic Resonance, 2021, 2, 447-464.	0.8	7
108	Resolution enhancement in 1D solid-state NMR spectra of spin-9/2 quadrupolar nuclei. Journal of Magnetic Resonance, 2006, 180, 311-316.	1.2	6

#	Article	IF	CITATIONS
109	Probing proximities between different quadrupolar isotopes using multi-pulse cross-polarization. Journal of Magnetic Resonance, 2013, 228, 148-158.	1.2	6
110	Evaluation of95Mo Nuclear Shielding and Chemical Shift of [Mo6X14]2–Clusters in the Liquid Phase. Inorganic Chemistry, 2015, 54, 7673-7683.	1.9	6
111	1 H- 31 P CPVC NMR method under Very Fast Magic Angle Spinning for analysis of dipolar interactions and dynamics processes in the crystalline phosphonium tetrafluoroborate salts. Solid State Nuclear Magnetic Resonance, 2017, 87, 96-103.	1.5	6
112	Rotor-synchronized dipolar-filter sequence at fast MAS in solid-state NMR. Journal of Magnetic Resonance, 2011, 212, 455-459.	1.2	5
113	Exploring various modulation-sideband recoupling conditions of SHA+ sequence at fast MAS. Solid State Nuclear Magnetic Resonance, 2013, 55-56, 42-47.	1.5	5
114	71 Ga- 77 Se connectivities and proximities in gallium selenide crystal and glass probed by solid-state NMR. Journal of Magnetic Resonance, 2017, 282, 71-82.	1.2	5
115	Combining heteronuclear correlation NMR with spin-diffusion to detect relayed Cl–H–H and N–H–H proximities in molecular solids. Solid State Nuclear Magnetic Resonance, 2022, , 101808.	1.5	5
116	Measurement of the shortest hetero-nuclear distances in multiple-spin systems using constant-time correlation NMR methods. CrystEngComm, 2013, 15, 8713.	1.3	4
117	3D correlation NMR spectrum between three distinct heteronuclei for the characterization of inorganic samples: Application on sodium alumino-phosphate materials. Solid State Nuclear Magnetic Resonance, 2017, 84, 164-170.	1.5	4
118	Local measure of the electromagnetic field in magnetic resonance coils: How do simulations help to disentangle the contributions of the electric and magnetic fields?. Solid State Nuclear Magnetic Resonance, 2017, 82-83, 1-9.	1.5	4
119	Forcing the â€~lazy' protons to work. Physical Chemistry Chemical Physics, 2018, 20, 25829-25840.	1.3	4
120	Synthesis, Crystal and Electronic Structures, and Magnetic Properties of LiLn <sub>9</sub> Mo <sub>16</sub> O <sub>35</sub> (Ln=La, Ce, Pr, and Nd) Compounds Containing the Original Cluster Mo <sub>16</sub> O <sub>36</sub> . Chemistry - A European Journal, 2011, 17, 13806-13813.	1.7	3
121	Glass to crystal transformation in the ternary BaO Nb 2 O 5 P 2 O 5 system. Journal of Molecular Structure, 2017, 1143, 472-477.	1.8	3
122	Recording 13C-15N HMQC 2D sparse spectra in solids in 30â€⁻s. Journal of Magnetic Resonance, 2018, 288, 76-83.	1.2	3
123	Simple and Robust Study of Backbone Dynamics of Crystalline Proteins Employing <sup>1</sup> H– <sup>15</sup> N Dipolar Coupling Dispersion. Journal of Physical Chemistry B, 2018, 122, 8146-8156.	1.2	3
124	Rationalization of solid-state NMR multi-pulse decoupling strategies: Coupling of spin l = ½ and half-integer quadrupolar nuclei. Journal of Magnetic Resonance, 2019, 303, 48-56.	1.2	3
125	Throughâ€space 11 B– 27 Al correlation: Influence of the recoupling channel. Magnetic Resonance in Chemistry, 2021, 59, 1062-1076.	1.1	3
126	gem â€Ðiolâ€Type Intermediate in the Activation of a Ketone on Snâ€Î² Zeolite as Studied by Solidâ€&tate NMR Spectroscopy. Angewandte Chemie, 2020, 132, 19700-19706.	1.6	2

#	Article	IF	CITATIONS
127	Probing 29Si-17O connectivities and proximities by solid-state NMR. Journal of Magnetic Resonance, 2021, 330, 107029.	1.2	2
128	Hadamard acquisition of 13 C– 13 C 2â€Ð correlation NMR spectra. Magnetic Resonance in Chemistry, 2021, 59, 247-256.	1.1	1